Study of Strange Matter in STAR with Express Analysis

Ivan Kisel[1,2,3,4,*], for the STAR Collaboration

[1]Goethe University, Frankfurt am Main, Germany
[2]FIAS, Frankfurt Institute for Advanced Studies, Frankfurt am Main, Germany
[3]HFHF, Helmholtz Research Academy Hesse, Frankfurt am Main, Germany
[4]GSI, Helmholtz Center for Heavy Ion Research, Darmstadt, Germany

Abstract. The STAR experiment provides a perfect machinery for studying strange matter for more than two decades. Recently, we developed the express stream procedure, which allows online monitoring of the collected physics data. The high quality of express calibration and reconstruction provides a unique possibility to run the express production and observe almost in real time strange particles including mesons, hyperons, resonances and even hypernuclei.
The STAR Beam Energy Scan II program, including fixed target Au+Au collisions taken in 2018–2021, is particularly suited to study hypernuclei. Light hypernuclei are expected to be abundantly produced in low energy heavy-ion collisions. Measurements of hypernuclei production and their properties will provide information on the hyperon-nucleon interactions, which are essential ingredients for understanding nuclear matter equation of state at high net-baryon densities, such as inside neutron stars.
With the heavy fragment trigger introduced for the 2021 data taking, we were able to run the express stream production at the STAR High Level Trigger farm. The collected data were sufficient to observe the decay process of ${}^{5}_{\Lambda}\mathrm{He} \rightarrow {}^{4}\mathrm{He}p\pi^{-}$ with more than 11σ significance, measure binding energy as a function of hypernuclei mass, and study hypernuclei decay properties with the Dalitz plot technique.

1 Introduction

Since hyperons are elementary particles containing at least one *s*-quark, but do not contain the heavier *c* and *b* quarks, i.e., they consist of three light quarks, at least one of which is an *s*-quark, hyperons are formed in large amounts during collisions of heavy ions, which allows one to study their properties in detail with heavy ion experiments.

The formation of hyperons in large amounts also makes it possible to study hypernuclei, which are a system of strongly interacting particles consisting of nucleons (protons and neutrons) and one or more hyperons. The structure of hypernuclei is determined by nuclear interaction between nucleons and hyperons.

Hypernuclei are excellent experimental probes for studying hyperon-nucleon (Y-N) interactions. The Y-N interaction is an important component in the description of the hadronic phase of heavy ion collisions, as well as in the equation of state (EoS) of astrophysical objects, such as neutron stars [1]. Therefore, heavy ion collisions at RHIC provide a unique

*e-mail: I.Kisel@compeng.uni-frankfurt.de

opportunity to study also the Y-N interaction in finite temperature and density regions by measuring the hypernuclear lifetime, production yield, etc.

In this publication, we present preliminary results from a real-time search for hyperons and hypernuclei using an express data stream on a computer cluster of the High Level Trigger (HLT) in the STAR experiment within the Beam Energy Scan phase-II (BES-II) program (2018–2021) [2].

2 Extended functionality of the High Level Trigger for BES-II

In order to create a package of algorithms for full processing and analysis of data in real time within the BES-II physics program, the functionality of the HLT computer cluster was significantly extended. This was done within the FAIR Phase-0 program, which allowed adapting the package of fast algorithms for processing and analysis FLES (First Level Event Selection) [3] of the CBM experiment (FAIR/GSI) data to work with real data of the STAR experiment.

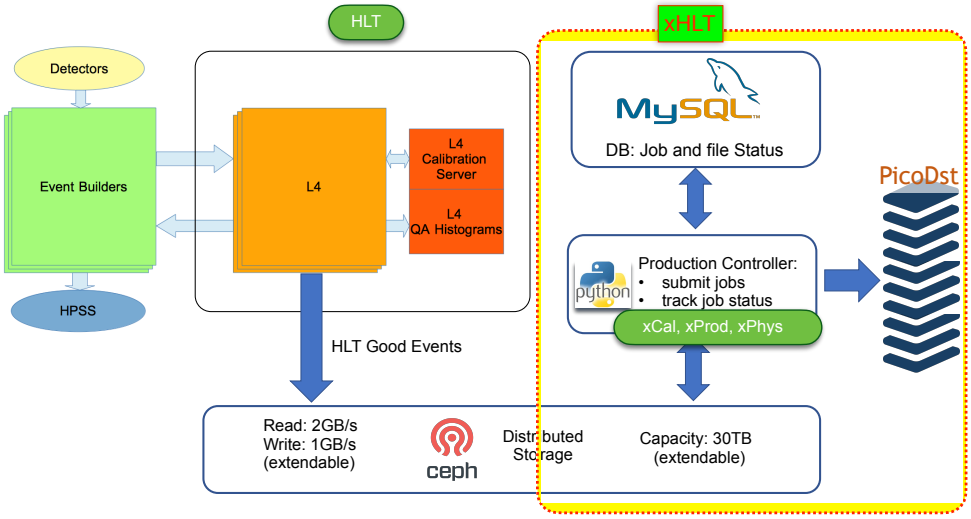

Figure 1. Full chain of express production and analysis has been running on STAR HLT since 2019.

Basic elements of data processing and analysis are search of particle trajectories in the detector system based on the Cellular Automaton (CA Track Finder) and search of short-lived particles based on the Kalman filter method (KF Particle Finder) [3]. These algorithms, after careful adaptation and detailed testing on simulated data, were checked with the Au+Au collisions recorded in 2014, 2016, and BES-I. It was shown that using the CA Track Finder provides 25% more D^0 and 20% more W when processing a sample of pp collisions at 510 GeV collected in 2013. Also, the KF Particle Finder package provides twice as many signal particles with the same background level as the standard approach used in STAR. The reliability and high performance of both algorithms allowed them to be included in the real-time express physics analysis chain at the HLT computer cluster during the BES-II (2018-2021) runs.

It is also essential that a data calibration package, optimized for real-time operation, has been added to the HLT operation. This package has shown an exceptionally high performance with BES-II data, which resulted in high quality of the CA Track Finder, as well as in

the KF Particle Finder's accurate search for short-lived particles, in particular hyperons and hypernuclei.

3 BES-II: Search for mesons and hyperons

The quality of the express chain of data processing and analysis was continuously tested in real time using meson reconstructions as an example.

Table 1. Results of the search for mesons and hyperons in the STAR HLT express data stream.

Decay	Mass, MeV/c^2	σ, MeV/c^2	S	S/B	$S/\sqrt{S+B}$
$\pi^0 \to \gamma_{e^+e^-}\gamma_{e^+e^-}$	135.9	4.2	$14.0 \cdot 10^3$	0.2	48
$K_s^0 \to \pi^+\pi^-$	497.3	4.1	$67.1 \cdot 10^6$	6.5	7629
$K_s^+ \to \pi^+\pi^+\pi^-$	493.9	2.6	$2.4 \cdot 10^6$	24.3	1524
$K_s^- \to \pi^+\pi^-\pi^-$	493.9	2.4	$0.7 \cdot 10^6$	8.3	839
$K_s^+ \to \pi^+\pi^+\pi^-$ + K track	493.8	2.0	$35.7 \cdot 10^3$	inf	189
$K_s^- \to \pi^+\pi^-\pi^-$ + K track	493.8	2.0	$12.9 \cdot 10^3$	inf	114
$\pi^+ \to \mu^+\nu_\mu$	138.2	2.2	$2.1 \cdot 10^6$	75.9	1443
$\pi^- \to \mu^-\bar{\nu}_\mu$	138.2	2.2	$2.4 \cdot 10^6$	78.6	1546
$K^+ \to \mu^+\nu_\mu$	493.8	9.1	$3.1 \cdot 10^6$	4.7	1606
$K^- \to \mu^-\bar{\nu}_\mu$	493.6	9.0	$1.1 \cdot 10^6$	4.5	956
$K^+ \to \pi^+\pi^0$	493.2	6.7	$1.0 \cdot 10^6$	2.6	830
$K^- \to \pi^-\pi^0$	493.1	6.6	$0.3 \cdot 10^6$	2.4	489
$\Lambda \to p\pi^-$	1115.7	1.5	$60.1 \cdot 10^6$	24.6	7601
$\bar{\Lambda} \to \bar{p}\pi^+$	1115.7	1.4	$0.9 \cdot 10^6$	7.1	931
$\Xi^- \to \Lambda\pi^-$	1321.9	2.1	$0.8 \cdot 10^6$	21.8	890
$\bar{\Xi}^+ \to \bar{\Lambda}\pi^+$	1321.9	2.1	$45.8 \cdot 10^3$	36.7	211
$\Omega^- \to \Lambda K^-$	1672.4	2.2	$9.2 \cdot 10^3$	3.9	86
$\bar{\Omega}^+ \to \bar{\Lambda}K^+$	1672.4	2.4	$2.2 \cdot 10^3$	12.0	46

The upper part of table 1 shows the results of reconstruction of decay channels $\pi^0 \to \gamma_{e^+e^-}\gamma_{e^+e^-}$, $K_s^0 \to \pi^+\pi^-$, $K_s^+ \to \pi^+\pi^+\pi^-$ and $K_s^- \to \pi^+\pi^-\pi^-$ after processing 140M Au+Au events at 7.7 GeV, collected in 2021. Due to the high quality of online calibration and processing, strange mesons are reconstructed with high significance and S/B ratio, and even π^0 is observed with a significant of 48σ. Reconstruction of π^0 relies on a rather complex search of photons, as electron and positron are parallel at the conversion point, and requires high efficiency of track finding, since 4 tracks are produced in the decay tree.

Also there is an example of processing 32.5M Au+Au events at 7.7 GeV to search for decays $K_s^+ \to \pi^+\pi^+\pi^-$ and $K_s^- \to \pi^+\pi^-\pi^-$ when all four tracks are registered in the detector system and reconstructed. STAR with its perfectly working TPC detector allows to identify charged kaons without background by full topological reconstruction with all 4 tracks. Reconstruction of such full decay topologies provides additional technical opportunities to study quality of detector performance and reconstruction algorithms.

Decay channels of pions and kaons with a neutral daughter particle can also be found using the missing mass method. The middle part of table 1 shows the results of the reconstruction of decay channels $\pi^+ \to \mu^+\nu_\mu$, $\pi^- \to \mu^-\bar{\nu}_\mu$, $K^+ \to \mu^+\nu_\mu$, $K^- \to \mu^-\bar{\nu}_\mu$, $K^+ \to \pi^+\pi^0$ and $K^- \to \pi^-\pi^0$ after processing 32.5M Au+Au events at 7.7 GeV, collected in 2021. The missing mass method provides various opportunities in the study of different decay channels with a neutral daughter particle.

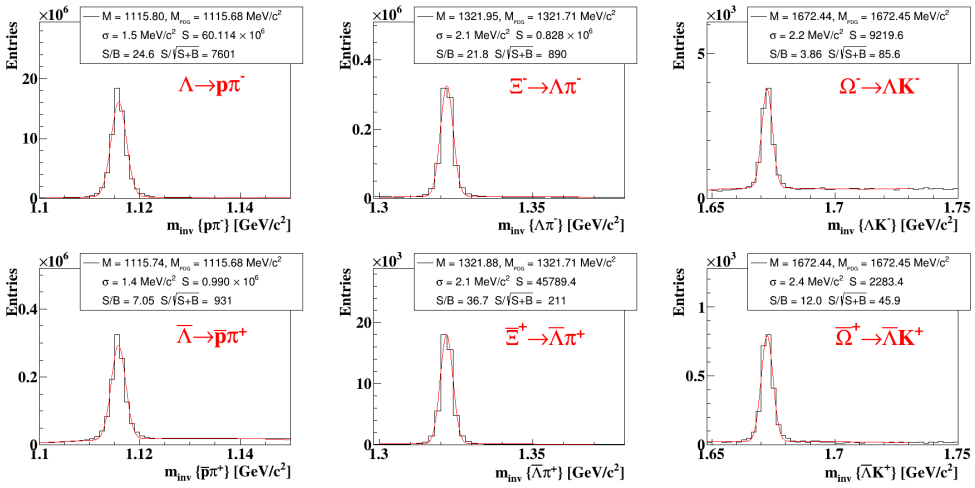

Figure 2. With express calibration and production we observe in real time all hyperons with high significance and S/B ratio.

STAR has recently upgraded the inner part of the TPC, which, together with the enhanced CA track finder, has improved the efficiency of hyperon reconstruction. The bottom part of table 1 and Fig. 2 show the results of reconstruction of the hyperon decay channels after processing 140M Au+Au events at 7.7 GeV, collected in 2021. It can be seen that the high quality of the new BES-II experimental data provides an excellent opportunity to study hyperons.

4 BES-II: Search for hypernuclei

In order to increase statistics of the experimental data set for the search of hypernuclei at the lowest energy of 3.0 GeV in the BES-II program, intensity of the beam collision in the fixed-target mode was significantly increased. This led to that more than half of the events in the STAR detector consist of at least two closely overlapping heavy ion collisions, i.e., after reconstruction the events had two or more reconstructed primary vertices. This required a more detailed data analysis within the KF Particle Finder package to detect and carefully clean up interactions of beam particles with the beam pipe material and support structures. Such a cleaning procedure involved, among other things, reconstruction of multiple primary vertices from interactions with the beam pipe and support structures as well as the pileup events, and then discarding such found primary tracks. This cleaning procedure reduced significantly the background in hypernuclei spectra, especially in three-body channels, compared to the standard procedure used at higher energies and lower intensities.

Another feature of the search for hypernuclei was that as the intensity of the beam increased in the fixed-target mode, the HLT computer cluster did not have enough resources to process and analyze all the collected data online. Therefore, in order to fully process the data with the goal of searching for hypernuclei, a trigger was introduced, requiring the presence of a He nucleus in the event, for subsequent real-time analysis. A set of 437M triggered Au+Au collisions at $\sqrt{s_{NN}}$ = 3.0 GeV in the fixed-target mode recorded in 2021 on HTL proved to be sufficient to measure the yield, lifetime, and spectra of the hypernuclei.

Using the same procedure, the 7.7 GeV data in the collider mode collected in 2021 were also analyzed within the express chain, as well as data sets of different energies in the fixed-

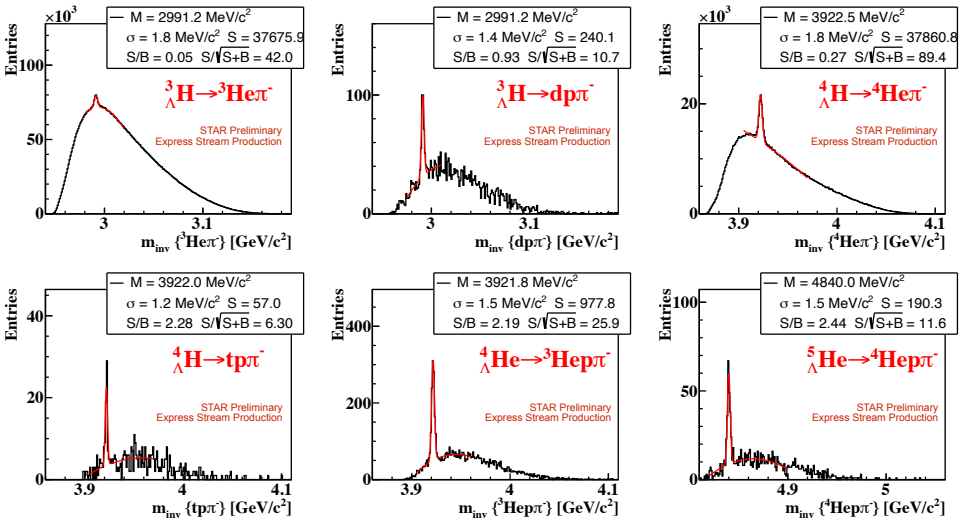

Figure 3. Standard and express reconstruction of hypernuclei using 2018, 2019, 2020, and 2021 data collected at different energies in the collider and fixed-target modes. The signal of ${}^{5}_{\Lambda}$He is visible with a significance of 11.6σ.

target mode collected in 2018, 2019, and 2020 and processed with the STAR standard production chain after the final calibration. After such (express and standard) processing of all the data, the signal of the ${}^{5}_{\Lambda}$He hypernucleus is clearly visible with a significance of 11.6σ (see Fig. 3).

Collected statistics are also sufficient to study Dalitz plots in the 3-body decay channels. Thus, Figs. 4 and 5 show the Dalitz plots for the decay ${}^{4}_{\Lambda}$He $\rightarrow$ ^{3}He+p+π^{-} which has the largest number of signals (978 decays) found. The background was estimated using the side-band method and subtracted under the peak. As can be seen, the background is smooth and no structures are observed. The complex structure in the pπ projection can be explained as a possible spin effect. In the nucleus-p combination, the signal and the background show different behavior. There can be seen a hint of two-body ^{4}Li π^{-} decay (^{4}Li (J^{P} = 2^{-}): M = 3.75 GeV/c^{2}, σ = 8.7 MeV/c^{2}). Similar behavior is observed in the Dalitz plots for the decays of hypernuclei ${}^{5}_{\Lambda}$He $\rightarrow$ ^{4}He+p+π^{-} and ${}^{3}_{\Lambda}$He $\rightarrow$ d+p+π^{-}, but with lower statistics, 190 and 240 signal particles, respectively.

As for the binding energy of the hypernuclei (Fig. 6), one can see that it increases for heavier hypernuclei up to ${}^{5}_{\Lambda}$He. When comparing binding energies per nucleon, hypernuclei behave similarly to ordinary nuclei (see Table 2). Thus, the value of the binding energy per nucleon in the hypernuclei, together with hints of their two-body resonance decays, may be an indication that Λ in the hypernuclei behaves similarly to other nucleons, n and p.

Table 2. Hypernuclei behave similarly to ordinary nuclei with respect to the binding energy per nucleon.

${}^{5}_{\Lambda}$He	6.30 MeV/c^{2}	^{4}He	7.07 MeV/c^{2}	^{5}He	5.48 MeV/c^{2}	^{5}Li	5.27 MeV/c^{2}
${}^{4}_{\Lambda}$He	2.55 MeV/c^{2}	^{3}He	2.57 MeV/c^{2}	^{4}He	7.07 MeV/c^{2}	^{4}Li	1.15 MeV/c^{2}
${}^{4}_{\Lambda}$H	2.65 MeV/c^{2}	^{3}H	2.83 MeV/c^{2}	^{4}H	1.40 MeV/c^{2}		
${}^{3}_{\Lambda}$H	0.8-0.9 MeV/c^{2}	^{2}H	1.11 MeV/c^{2}	^{3}H	2.83 MeV/c^{2}		

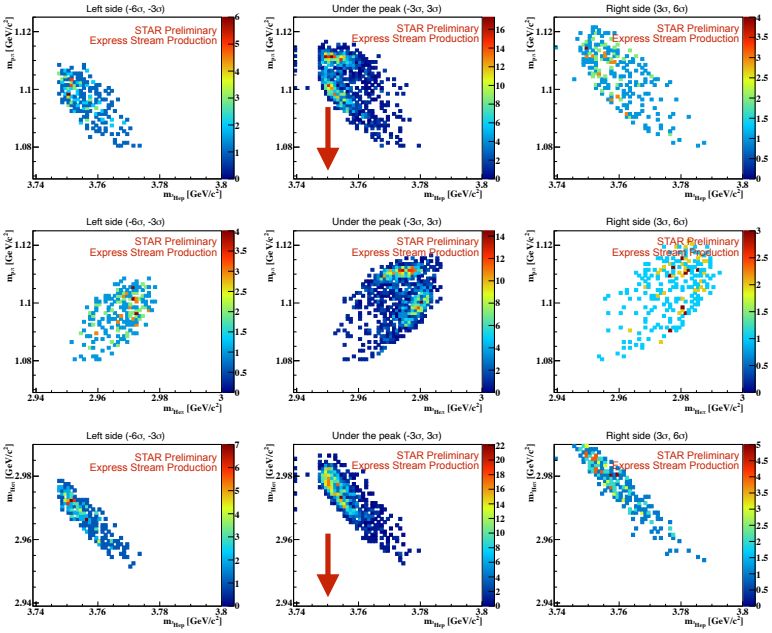

Figure 4. The Dalitz plots for the decay ${}^{4}_{\Lambda}\mathrm{He} \rightarrow {}^{3}\mathrm{He}+\mathrm{p}+\pi^{-}$ which has the largest number of signals (978 decays) found using 2018, 2019, 2020, and 2021 data collected at different energies in the collider and fixed-target modes.

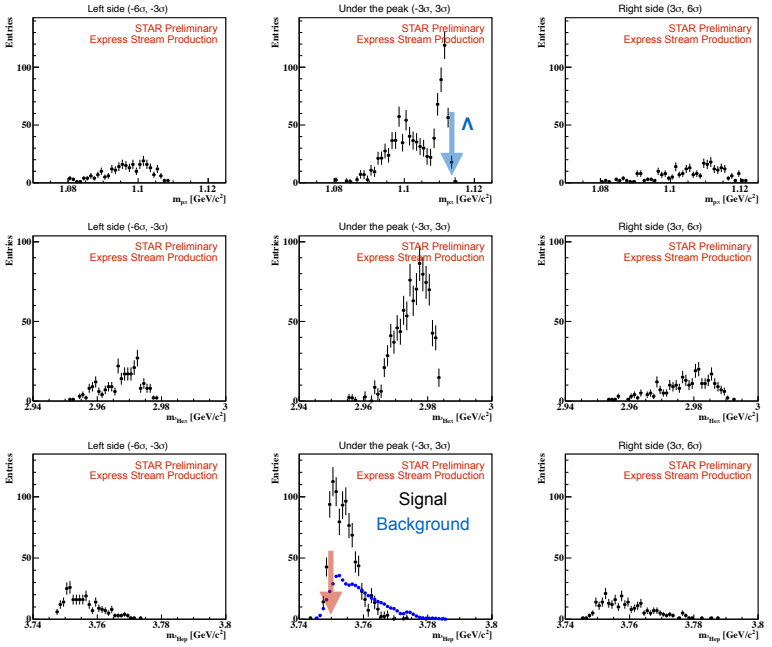

Figure 5. Projections of the Dalitz plots for the decay ${}^{4}_{\Lambda}\mathrm{He} \rightarrow {}^{3}\mathrm{He}+\mathrm{p}+\pi^{-}$. The complex structure in the signal in the pπ projection can be explained as a possible spin effect. In the nucleus-p combination, the signal and the background show different behavior. There can be seen a hint of two-body ${}^{4}\mathrm{Li}$ π^{-} decay (${}^{4}\mathrm{Li}$ ($J^{P} = 2^{-}$): M = 3.75 GeV/c^{2}, σ = 8.7 MeV/c^{2}).

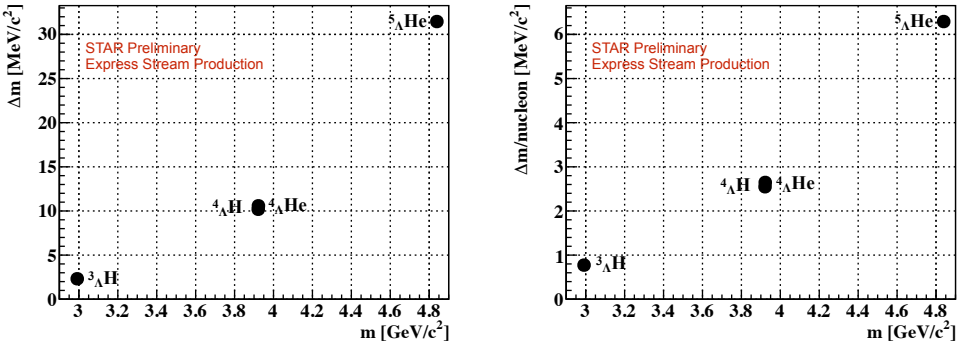

Figure 6. The binding energy of the hypernuclei increases for heavier hypernuclei up to ${}^{5}_{\Lambda}$He. Only statistical errors are shown, which are smaller than the symbol size.

5 Conclusion

During processing and analysis of express stream data on the STAR HLT within the BES-II program in 2018–2021 the reconstruction of particle trajectories was done in real time by the track finder based on the Cellular Automaton, and the search for short-lived particles and hypernuclei by the KF Particle Finder package based on the Kalman filter.

Throughout the data acquisition of the BES-II physics program operation, real-time data analysis showed high quality of the experimental data collected by the STAR detector. The online processing of the express stream data on the STAR HLT farm showed excellent signatures ranging from mesons to hypernuclei. High quality of the collected experimental data and online calibration, and reliable performance of data processing and analysis algorithms allowed us to observe and investigate various hypernuclei up to ${}^{5}_{\Lambda}$He with a significance of 11.6σ. The Dalitz plots of three-body decays of hypernuclei show complex structures with the possible presence of spin effects. There are also hints that a significant fraction of such three-body decays happen via nuclear resonances.

The binding energy per nucleon in hypernuclei increases with increasing A up to ${}^{5}_{\Lambda}$He. There are indications that Λ behaves similarly to other nucleons, n and p, in hypernuclei. Theoretical models of the hypernuclei decays are needed to make a more detailed analysis of the efficiency of three-body decay channels and branching ratios.

6 Acknowledgements

The author considers it his duty to express his gratitude to the entire STAR Collaboration, and especially to the members of STAR HLT/TFG Group Y. Fisyak, H. Ke, S. Margetis, A. Tang, I. Vassiliev and M. Zyzak for their enormous work in obtaining the results given in the paper.

References

[1] J. Steinheimer et al., Phys. Lett. **B 714**, 85 (2012).
[2] Q. Yang (for the STAR Collaboration), Nucl. Phys. **A 982**, 951 (2019).
[3] I. Kisel, (CBM, STAR collaborations), J. Phys. Conf. Ser. **1602**, 012006 (2020).